Mechanism of B diffusion in crystalline Ge under proton irradiation

E. Bruno,* S. Mirabella, G. Scapellato, G. Impellizzeri, A. Terrasi, and F. Priolo
MATIS CNR-INFM and Dipartimento di Fisica e Astronomia, Università di Catania, Via S. Sofia 64, 95123 Catania, Italy

E. Napolitani, D. De Salvador, M. Mastromatteo, and A. Carnera
MATIS CNR-INFM and Dipartimento di Fisica, Università di Padova, Via Marzolo 8, 35131 Padova, Italy
(Received 15 June 2009; published 15 July 2009)

B diffusion in crystalline Ge is investigated by proton irradiation in thin layers with B delta doping under different fluences (1×10^{15}–10×10^{15} H^+/cm^2), fluxes (6×10^{11}–35×10^{11} H^+/cm^2 s), and temperatures of the implanted target (from −196 to 550 °C), both during and after irradiation. B migration is enhanced by several orders of magnitude with respect to equilibrium. Moreover, B diffusion is shown to occur through a point-defect-mediated mechanism, compatible with a kick-out process. The diffusion mechanism is discussed. These results are a key point for a full comprehension of the B diffusion in Ge.

DOI: 10.1103/PhysRevB.80.033204 PACS number(s): 66.30.−h, 68.55.Ln, 61.72.−y

Silicon and germanium, very similar from crystallographic and electronic points of view, appear to be quite different as far as the dopant behavior is concerned. In Si dopants of the III and V groups diffuse by a point-defect (PD) mediated mechanism that can involve both vacancies (*V*s) and self-interstitials (*I*s), prevailing the former or the latter mechanism depending on the considered dopant.[1,2] In contrast, in Ge almost all dopants seem to diffuse by a *V*-mediated mechanism. This is attributed to the determination that *V*s in Ge play a dominant role with respect to *I*s since *V*s are characterized by a lower formation energy.[3] However, while the dopant properties in Si are now well assessed,[1] in Ge the picture is still controversial.[4] Germanium has been the first semiconductor in the microelectronic industry but was totally replaced by silicon in the 1960s and since then was almost abandoned. Recently, it is acquiring a strong renewed industrial and scientific interest[5–13] thanks to its higher carrier mobility, together with its high compatibility with the already existing Si-based technology. Nevertheless, since knowledge on this semiconductor has remained almost frozen for about 50 years, we still lack much basic information.

Boron is the most used *p*-type dopant in both Si and Ge. Nonetheless, if B diffusion in Si is deeply understood,[14–17] only a few data about B in Ge exist in the literature, most of which were made many decades ago, often carried out under poorly defined conditions and restricted to simple sheet resistivity and junction depth measurements, thus resulting in quite disagreeing diffusivity values.[18,19] Recently, B diffusivity in Ge has been measured under controlled conditions and a diffusion coefficient two orders of magnitude smaller than the smallest earlier estimate was determined.[5] B diffusivity appeared to be much smaller than the diffusivity of all the other dopants in Ge.[3,7] Indeed, its very high activation energy of 4.65 eV,[5,6] together with the theoretical instability of the B-*V* pair[9] or the very high activation energy for *V*-mediated B diffusion obtained by *ab initio* calculations,[10] suggest that B in Ge should diffuse by interacting with *I*s. This is supported indeed by the results of Carvalho *et al.*[20] pointing out that *I*s in Ge are more stable than in Si and are positively charged, thus favoring their interaction with the negatively charged substitutional B.

In addition, since B is such a slow diffuser, the experimental study of its migration mechanism is limited to a restricted range of very high temperatures and very long times. Thus, up to now no experimental studies are available for describing the B diffusion mechanism in Ge and the microscopic mechanism has not been experimentally proven. Hence, alternative approaches are in high demand in order to clarify the B diffusion process in Ge and how point defects can affect B diffusion itself.

In this Brief Report we present experimental investigation of B diffusion in crystalline Ge (*c*-Ge) under and after proton irradiation. The resulting radiation-enhanced diffusion of B was, hence, systematically studied, clarifying the migration mechanism of B in Ge.

A ⟨001⟩ Ge sample containing a 3-nm-thick B delta doped layer at a concentration level of 2×10^{18} B/cm^3 and placed at a depth of 550 nm was grown by molecular beam epitaxy (MBE). The B delta was used as a marker for B diffusion, as previously done in Si crystals.[17,21] All samples were preannealed at 600 °C for 1 h under N_2 atmosphere to eliminate any possible postgrowth defects. Then, samples were implanted with H^+ at 300 keV [projected range R_p of ~2.5 μm (Ref. 22)] at different fluences (1×10^{15}–10×10^{15} H^+/cm^2), fluxes (6×10^{11}–35×10^{11} H^+/cm^2 s), and at various temperatures [from the liquid-nitrogen temperature (LN_2T) up to 550 °C]. B chemical profiling was obtained by secondary-ion-mass spectrometry (SIMS) analyses performed at room temperature (RT) with a Cameca IMS-4 *f* instrument (3 keV O_2^+ analyzing beam). Some measurements were repeated in selected samples at −70 °C showing that, contrary to what was observed in Si,[23] sputtering by SIMS induces no significant migration of B at RT. This can be ascribed to the larger ion damage occurring in Ge with respect to Si, causing a complete amorphization of the Ge surface during the SIMS analyses, which hampers the injection of PDs.[24] In addition, scanning electron microscopy (SEM) analyses of selected crater bottoms (not shown) have excluded the onset of pits during SIMS measurements of our samples. Such pits, inducing significant distortion of SIMS profiles, have been observed during sputtering of Ge samples previously irradiated with proton beams at higher energies and fluxes than in our case.[12]

 ©2009 The American Physical Society

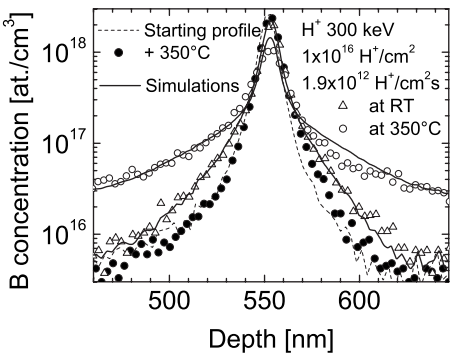

FIG. 1. Boron SIMS profiles in the starting sample (i.e., the as-grown sample after 600 °C for 1 h, dashed line), and after irradiation at RT (open triangles) and 350 °C (open circles) with H^+ 300 keV, 1.9×10^{12} H^+/cm^2 s and 1×10^{16} H/cm^2. A reference for thermal diffusion at 350 °C is also plotted (closed circles). Solid lines are simulations of the data based on the kick-out model.

In Fig. 1 we report the starting profile (i.e., the as-grown sample after 1 h of 600 °C annealing, dashed line), and the one after irradiation at RT (open triangles) and 350 °C (open circles) with the 300 keV H^+ ion beam, at an ion flux of 1.9×10^{12} H^+/cm^2 s with a fluence of 1×10^{16} H^+/cm^2. A not-implanted sample but annealed for the same total time at 350 °C is also plotted as a reference for the thermal diffusion at 350 °C (closed circles). It is evident how at high-T irradiation strongly enhances the B diffusion with respect to the negligible thermal diffusion. Surprisingly, even at RT boron strongly diffuses under irradiation (open triangles) well over the thermal diffusion at 350 °C. It is worth noting that, in contrast, when implanted at the LN_2T the B delta profile does not broaden at all (not shown), meaning that ion-assisted B diffusion needs to be thermally activated.

The diffused B profiles show a non-Gaussian shape, far away from those typical of the diffusion phenomena driven by the Fick's diffusion laws. Indeed, the exponential diffusion tails unambiguously demonstrate that the B diffusion mechanism in Ge is mediated by the formation of an intermediate mobile B complex, formed through the interaction of substitutional B atoms (B_s) with the PDs generated by the incident ion beam, in a fashion somewhat similar to what was observed in Si.[14,15] We thus propose in Ge a similar mechanism, where B_s becomes mobile (B_m) with a rate g by interacting with PDs (kick-out mechanism) and then B_m moves for a mean length λ before returning substitutional (i.e., immobile) with a rate r (kick-in mechanism). Thus, the B diffusivity can be expressed as $D_B=g\lambda^2$.

In order to quantitatively study the B diffusion phenomenon, we fitted the experimental profiles at different implant fluences, ion fluxes, and temperatures by means of a χ^2 optimization of simulations numerically generated according to a g-λ diffusion model as described in Refs. 14 and 15. The continuous lines in Fig. 1 accounts for the quality of all the fits obtained by the model. As an example, the values of g and λ obtained for the sample irradiated at 350 °C in Fig. 1 are of $(1.5\pm0.2)\times10^{-4}$ s^{-1} and 28 ± 4 nm, respectively.

In Fig. 2 g (closed squares), λ (closed circles), and gt (closed diamonds) are reported (where t is the diffusion time)

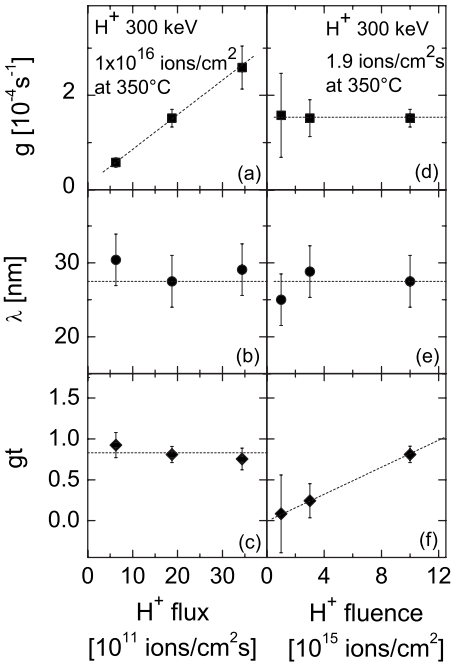

FIG. 2. Values of g (closed squares), λ (closed circles), and gt (closed diamonds, where t is the diffusion time) are reported as a function of the H^+ flux [Figs. 2(a)–2(c)] and $^+$ fluence [Figs. 2(d)–2(f)] for samples implanted at 350 °C, by fixing the fluence at 1×10^{16} H^+/cm^2 or the flux at 1.9×10^{12} H^+/cm^2 s, respectively. The dashed lines are guidelines for the eye.

as a function of the H^+ flux [Figs. 2(a)–2(c)] and of the H^+ fluence [Figs. 2(d)–2(f)] for samples implanted at 350 °C, by fixing the H^+ fluence at 1×10^{16} H^+/cm^2 or the flux at 1.9×10^{12} H^+/cm^2 s, respectively. The dashed lines are guidelines for the eye. Figures 2(a) and 2(d) show that the B_m generation rate g linearly increases with the ion flux while it remains substantially constant by increasing the H^+ fluence. Instead, the migration path λ of B_m is unaffected by both the H^+ flux [Fig. 2(b)] and fluence [Fig. 2(e)].

During ion implantation, PDs in excess with respect to the equilibrium are generated within each collision cascade. The I and V concentrations are then limited by their diffusion and subsequent annihilation, returning to the equilibrium value after a certain transient time. Since the defect-B interaction rate g is proportional to the PDs population, the linear trend of g in Fig. 2(a) can be ascribed to the action of uncorrelated collision cascades, each of which extinguishes before being spatially superimposed to another cascade. Indeed, this indicates that a steady state for PD population is never reached. In fact, under pure athermal beam-induced I and V generations, and diffusion-limited annihilation, the PD populations (and as a consequence g) in steady-state conditions should have increased with a square-root trend.[12] Thus, the total observed diffusion of the B delta is the sum of many uncorrelated transient phenomena due to the fraction of PDs that can interact with B before annihilating. Therefore, the total number gt of migration events per B atom in the diffusion time t (i.e., the implant time) only depends on the implanted fluence [Fig. 2(f)] while the ion flux simply changes the frequency of migration events [Fig. 2(c)].

Under the above picture, the measured λ is the projection of the mean-free path perpendicularly to sample surface made by a B atom under the effect of many independent collision cascades. It is straightforward that at a given temperature λ must be constant, independent of both fluxes and fluences, as clearly evidenced by the experimental data in Figs. 2(b) and 2(e). Moreover, the constant trend of λ for all the H^+-implanted fluences also demonstrates that the B diffusion process is not affected by the presence of H atoms. In fact, if any H diffusion from its R_p region occurred, different amount of H would be present around the B delta affecting λ. This is not the case.

It is worth noting that the observed B diffusion is certainly not due to a direct knock-on phenomenon on B atoms generated by the impinging ion beam. In fact, at 350 °C the threshold fluence to have each B atom involved in at least one migration event (i.e., to have $gt \sim 1$) is $\sim 1 \times 10^{16}$ H^+/cm^2 [Fig. 2(f)]. On the other hand, if we calculate the displacements per Ge atom in Ge after a 300 keV 1×10^{16} H^+/cm^2 implantation at the depth of the B delta, we obtain $\sim 1 \times 10^{-2}$ (Ref. 22). Indeed, the displaced B atoms for the same H^+ implant would be even much lower because the knock on inversely depends on the square of the atomic number. Thus, such calculations confirm our assumption that the observed broad B profiles are due to B diffusion indirectly caused by the interaction of B with the PDs generated by the implant.

Other fundamental information comes by investigation of diffusion parameters as a function of T. In Figs. 3(a)–3(c) the Arrhenius plots of the B diffusivity D_B (closed triangles), the migration rate g (closed squares), and the migration path λ (closed circles) are, respectively, reported for the samples implanted with 1×10^{16} H^+/cm^2 and 1.9×10^{12} H^+/cm^2 s versus T. Continuous lines are fits to the data. It is well evident from Fig. 3(a) that under H^+ irradiation B diffusivity is many orders of magnitude higher than the equilibrium one extracted by Uppal and co-workers[5] at T higher than 800 °C and here extrapolated at lower T [dashed line in Fig. 3(a)]. We also measured on these samples a thermal equilibrium D_B value at 755 °C (open triangle) in good agreement with Ref. 5. Note that, to obtain this point, annealing with times as long as 90 h were necessary. Under irradiation D_B shows a weak dependence on the T, characterized by a very low (almost athermal) activation energy of $E_D = 0.10 \pm 0.01$ eV. This can be understood considering the different diffusion steps by which B moves under the assumption that its diffusion is defect mediated and, hence, $D_B = g\lambda^2$.

The migration rate g [Fig. 3(b)] shows a single Arrhenius slope with a very low activation energy ($E_g = 0.06 \pm 0.01$ eV). The essentially athermal behavior of g can be explained considering that it results as a balance among different phenomena. Under the assumption that B diffuses by interacting with Is, g is a measure of the probability of I-B interaction forming the B-I pair and, therefore, it depends on the amount and diffusivity of Is. Interstitials are athermally generated by the ion beam while resulting more mobile at higher T. This increases the kick-out probability. On the other hand, it also favors the annihilation process $I + V \rightarrow \emptyset$, reducing the I concentration and, hence, the g value. Moreover, we cannot exclude that a small barrier for the formation of the B-I pair exists.

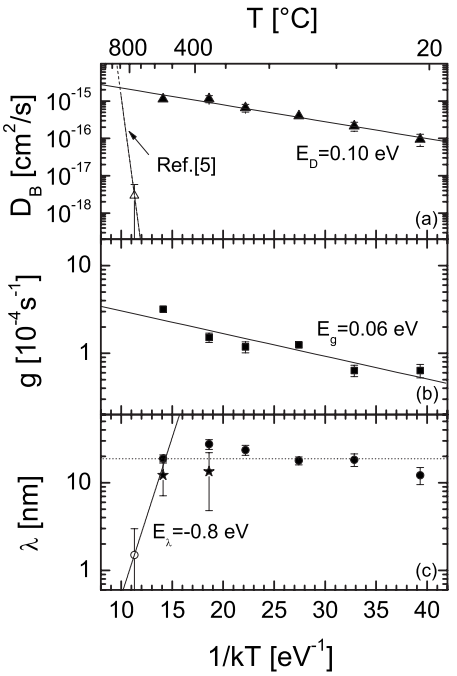

FIG. 3. Arrhenius plots of (a) D_B (closed triangles), (b) g (closed squares), and (c) λ (closed circles) for samples implanted with 1×10^{16} H^+/cm^2 and 1.9×10^{12} H^+/cm^2 s. Open symbols are relative to thermal diffusion. Stars are relative to diffusion under postimplant (1×10^{16} H^+/cm^2 and 1.9×10^{12} H^+/cm^2 s at RT) annealing. Dashed line in (a) is the thermal diffusivity extracted from Ref. 5. Dotted line in (c) is an eye guide. Continuous lines are fits of the experimental data. The activation energies obtained by the fitting process are reported.

It is worth noting that the absolute values of D_B and g in Figs. 3(a) and 3(b) could be scaled up and down by modifying the defect generation rate through the ion flux. In fact g, depending linearly on the ion flux [Fig. 2(a)], gives an ion-assisted diffusivity D_B, which is also a linear function of the flux ($D_B = g\lambda^2$).

Under proton irradiation, the migration length λ also shows a negligible dependence on T up to 550 °C [Fig. 3(c), the dotted line is an eye guide]. On the other hand, under equilibrium condition, at 755 °C we measured a value of λ [open circle in Fig. 3(c)], which is more than ten times lower than that observed under irradiation. The very high migration paths observed during the implants could be due to an ionization-enhanced diffusion of B occurring under irradiation through a more diffusive-charged mobile species, reminding that $\lambda = (D_{B_m}/r)^{1/2}$, as proposed in Si.[25] In fact, recently a charge-state-dependent diffusion has been also evidenced for Ga in Ge.[26] In order to ascertain if irradiation affects the B migration also through the free carrier generation, we studied the postimplant diffusion of B. In particular, the sample previously implanted at RT (1×10^{16} H^+/cm^2 and 1.9×10^{12} H^+/cm^2 s) was further annealed at 350 and 550 °C for 1 h. We clearly observed a postimplant-enhanced diffusion (not shown), similar to the well-known transient-enhanced diffusion of B in Si.[27] The observed enhanced diffusion can be ascribed to the PDs generated during the proton irradiation at RT and made mobile under the subsequent

annealing. However, since diffusion is now occurring without irradiation, ionization effects are absent. Indeed, the related migration paths [stars in Fig. 3(c)] are very close to those found under irradiation. This demonstrates that λ increases significantly by decreasing the T, independent of the presence of ionization effects. Moreover, the gt values measured at 550 and 350 °C after postimplant annealing (0.4 and 0.2, respectively) are a quarter of those under irradiation (1.7 and 0.8, respectively). Being gt the average number of migration events per B atom, this suggests that not all the PDs generated by the implant participate to the transient-enhanced B diffusion during the postimplant annealing, being partially annihilated during the implant itself or even during the annealing ramp.

The main point is that B migration path seems to increase noticeably by decreasing T. Similarly to what happens for B in Si,[15,17,25] we can assume that B diffusion stops through a dissociation process, for which λ increases by decreasing T with a similar mechanism in both equilibrium and nonequilibrium conditions. By fitting the data in the temperature range of 550–755 °C [continuous line in Fig. 3(c)], we obtain a negative activation energy for the kick-in process of ~−0.8 eV, very similar to the −0.5 eV observed for B in Si.[15] Nonetheless, at lower T, λ saturates at a value of ~20 nm. The peculiar quite constant behavior of λ over a very large range of the reciprocal temperature ($1/kT$ goes from 15 to 40 eV^{-1}) can be due to the presence of some kind of traps in the sample. We remind that all samples were preannealed at 600 °C to eliminate any possible postgrowth defects. Indeed, the observed values of the B migration path around 20 nm correspond to an average distance between traps having a concentration of $\sim 10^{17}$ cm^{-3}, a value comparable to the concentration of impurities such as O or C present in our MBE germanium sample. Thus, the presence of O and C could be a limiting factor for B migration when the distances covered by the mobile species overcomes the average distance among traps in the sample.

In conclusion, we demonstrated that under and after proton irradiation B suffers an enhanced diffusivity in c-Ge, many orders of magnitude higher than under equilibrium. B strongly diffuses even at RT under irradiation. Moreover, we demonstrated that B diffusion occurs through a mechanism mediated by PDs, through a kick-out mechanism followed by a subsequent thermally activated dissociation step of the mobile species (kick-in mechanism). The reported data are explained on the basis of an independent collision-cascade model. These results represent a fundamental point to achieve the elaboration of predictive atomistic diffusion models of B in c-Ge.

The authors wish to thank A. Irrera (MATIS CNR-INFM) for SEM analyses, C. Percolla and S. Tatì (MATIS CNR-INFM), and R. Storti (University of Padova) for technical expert assistance.

*elena.bruno@ct.infn.it

[1] H. Bracht, Mater. Res. Soc. Bull. **25**, 22 (2000), and references therein.
[2] U. Gösele *et al.*, Mater. Res. Soc. Symp. Proc. **610**, B7.1 (2000).
[3] J. Vanhellemont, P. Spiewak, and K. Sueoka, J. Appl. Phys. **101**, 036103 (2007), and references therein.
[4] C. Claeys and E. Simoen, *Germanium-Based Technologies - From Materials to Devices* (Elsevier, Amsterdam, 2007), and references therein.
[5] S. Uppal *et al.*, J. Appl. Phys. **96**, 1376 (2004).
[6] P. Delugas and V. Fiorentini, Phys. Rev. B **69**, 085203 (2004).
[7] A. Satta *et al.*, Appl. Phys. Lett. **87**, 172109 (2005).
[8] H. Bracht and S. Brotzmann, Mater. Sci. Semicond. Process. **9**, 471 (2006), and references therein.
[9] A. Chroneos, B. P. Uberuaga, and R. W. Grimes, J. Appl. Phys. **102**, 083707 (2007).
[10] C. Janke, R. Jones, S. Oberg, and P. R. Briddon, Phys. Rev. B **77**, 075208 (2008).
[11] S. Mirabella *et al.*, Appl. Phys. Lett. **92**, 251909 (2008).
[12] S. Schneider *et al.*, J. Appl. Phys. **103**, 033517 (2008).
[13] G. Impellizzeri *et al.*, J. Appl. Phys. **105**, 063533 (2009).
[14] N. E. B. Cowern, K. T. F. Janssen, G. F. A. van de Walle, and D. J. Gravesteijn, Phys. Rev. Lett. **65**, 2434 (1990).
[15] N. E. B. Cowern, G. F. A. van de Walle, D. J. Gravesteijn, and C. J. Vriezema, Phys. Rev. Lett. **67**, 212 (1991).
[16] B. Sadigh, T. J. Lenosky, S. K. Theiss, M. J. Caturla, T. Diaz de la Rubia, and M. A. Foad, Phys. Rev. Lett. **83**, 4341 (1999).
[17] D. De Salvador, E. Napolitani, S. Mirabella, G. Bisognin, G. Impellizzeri, A. Carnera, and F. Priolo, Phys. Rev. Lett. **97**, 255902 (2006).
[18] W. C. Dunlap, Jr., Phys. Rev. **94**, 1531 (1954).
[19] W. Meer and D. Pommerrenig, Z. Angew. Phys. **23**, 369 (1967).
[20] A. Carvalho, R. Jones, C. Janke, J. P. Goss, P. R. Briddon, J. Coutinho, and S. Oberg, Phys. Rev. Lett. **99**, 175502 (2007).
[21] S. Mirabella *et al.*, Phys. Rev. B **65**, 045209 (2002).
[22] J. F. Ziegler, J. P. Biersack, and U. Littmark, *The Stopping and Range of Ions in Solids*, Stopping and Ranges of Ions in Matter (Pergamon, New York, 1984), Vol. 1.
[23] E. Napolitani, D. De Salvador, R. Storti, A. Carnera, S. Mirabella, and F. Priolo, Phys. Rev. Lett. **93**, 055901 (2004).
[24] S. Koffel *et al.*, J. Appl. Phys. **105**, 013528 (2009).
[25] P. Leveque *et al.*, J. Appl. Phys. **89**, 5400 (2001).
[26] A. Mesli, L. Dobaczewski, K. B. Nielsen, V. Kolkovsky, M. C. Petersen, and A. N. Larsen, Phys. Rev. B **78**, 165202 (2008).
[27] S. C. Jain *et al.*, J. Appl. Phys. **91**, 8919 (2002).